Potential Planimetric Accuracy of Single IKONOS Imagery

By

Prof. Dr. Ahmed A. Shaker Dr. Mohamed I. Zahran
Dr. Youssef A. Youssef
Department of Surveying Engineering, Shoubra Faculty of Engineering, Zagazig University

ملخص البحث

ظهر في الآونة الأخيرة جيل جديد من أقمار التصوير الصناعية والتي تتميز بقدرتها التحليلية العالية. وتبرز من هذا الجيل الأقمار الصناعية "EarlyBird" و "QuickBird" و "OrbView-1" وأخيرا القمر الصناعي "IKONOS". وهذا الجيل من الأقمار يقدم صورا أرضية ذات قدرة تحليلية تصل إلى ١م ويتميز بمرونة عالية في توجيهه وكفاءة عالية في نظامه الاستشعاري ، مما يجعل هذه الأقمار مصدر اقتصادي هام لتوفير البيانات للعديد من التطبيقات في مجالات المسح التصويري والاستشعار عن بعد.

يقدم هذا البحث محاولة لدراسة الدقة البلانيمترية التي يمكن الحصول عليها من صور القمر الصناعي "IKONOS". لذا تم اختيار مجموعة من النقط المميزة في إحدى صور هذا القمر لمنطقة المعادي بالقاهرة وهي صورة أحادية اللون وذات قدرة تحليلية ١م. ولقد قيست إحداثيات هذه النقط في الصورة باستخدام إحدى برامج معالجة الصور الرقمية وقيست إحداثياتها الأرضية باستخدام محطة الرصد المتكاملة. وقد تم استخدام ثلاث نماذج لتحويل الإحداثيات لحساب دقة الإحداثيات البلانيمترية للنقط المختارة في الصورة. كذلك فقد تم تقويم دقة القياسات الخطية بمقارنة المسافات بين النقط المختارة والمستنتجة من الإحداثيات المقاسة علي الصورة ومن الإحداثيات المحولة بالمسافات المستنتجة من الإحداثيات الأرضية المناظرة. وطبقا للنتائج المستخلصة فقد وصلت دقة الإحداثيات البلانيمترية للنقط المميزة جيدا علي الصورة إلى أقل من ١م. ولقد تبين أيضا أنه بالرغم من أن نموذج التحويل (Similarity transformation) يتطلب الحد الأدنى من النقط المعلومة فانه يعطي نتائج تكاد تكون مكافئة لنظائرها في نماذج التحويل الأخرى.

Abstract

Several high-resolution imaging satellites have been launched recently. For example, EarlyBird and QuickBird from EarthWatch Inc., OrbView-1 from Orbital Science Corporation, and IKONOS from Space Imaging. The new generation of commercial satellites produces high-resolution imagery (up to 1 m), has flexible pointing ability and employs sensors of high geometric fidelity. This would provide a cost-effective source

of valuable information for numerous applications and revolutionize the work in photogrammetric and remote sensing domains.

This paper presents a study of the potential of the attainable planimetric accuracy of ground points from single IKONOS imagery. The test image is a panchromatic IKONOS digital image of 1m resolution for Maadi district, Cairo. A set of well-identified twelve feature points is selected carefully in the test image. The image coordinates of selected points are measured in the pixel coordinate system using image-processing software. Their object coordinates are obtained in an arbitrary ground coordinate system using the Total Station Sokki Set 2C.

Three transformation models are utilized to assess the planimetric coordinate accuracy of a set of selected feature points in the test image. In addition, the accuracy of linear measurements in the image is evaluated by testing image distances derived among the feature points against their corresponding ground distances. According to the test results, the planimetric coordinate accuracy of well-defined feature points in the test image reaches a magnitude that is less than the image resolution. It is found also that although Similarity transformation requires less control, it gives almost equivalent results comparing with affine and projective transformations.

1. Introduction

Several commercial companies scheduled launches of high-resolution imaging satellites in the late 90's. EarlyBird, which has 3m resolution, has been launched by EarthWatch Inc. in early 1998 but failed two-way communication. The company has operated also QuickBird that has 1m/4m resolution. OrbView-1 has been developed by Orbital Science Corporation and has1m/2m resolution. IKONOS (1m resolution) has been launched by SpaceImaging/EOSAT in late 1999.

In producing national map products, airborne photography is currently the primary technique employed. In spite of its advantages, such as high accuracy and flexible schedule, it can not map areas where airplanes can not reach. Also, its mapping frequency is constrained by the limits of flight planning. On the other hand, satellite

imagery makes it possible to map an area frequently without the special flight planning and scheduling required by aerial photogrammetric data acquisition. High-resolution satellite imagery have the potential for automatically extracting geographic information with the level of accuracy required by medium- and large-scale national digital mapping projects [2,5,6].

Satellite imagery has several advantages. Digital data gathered by a satellite sensor can be transmitted over radio or microwave communications links and stored on magnetic tapes, so they are easily processed and analyzed by a computer. Once the satellite is launched, the cost for data acquisition is less than that for aircraft data. Most importantly, satellites have very stable geometry, meaning that there is less chance for distortion or skew in the final image [7].

A satellite system is composed of a scanner and a satellite platform. The sensors are made up of detectors. The scanner is the entire data acquisition system. It embodies a sensor with detectors. A sensor is an instrument that gathers energy, converts it to a signal, and presents it in a form suitable for obtaining information about the environment [4]. Detectors are tiny devices in a sensor system that records electromagnetic radiation. Depending on the designed sensitivity of the detectors, sensors can measure reflectance of energy in the visible, near infrared, short wave infrared, thermal infrared, microwaves, and radar portions of the electromagnetic spectrum. The total width of the area on the ground covered by the scanner is called the swath width, or width of the total field of views (FOV). The FOV is a measure of the field of view of all detectors combined. It varies from a few kilometers for high-resolution satellites to thousands of kilometers for low-resolution satellites.

All civilian remote sensing satellites turn around the globe in near-polar orbits travelling in a slightly northeast-to-southwest direction on descending orbits which takes them almost directly over the poles on each orbit. Satellites orbit at constant speeds and altitude on predefined schedules. Satellite sensors can have either a fixed or adjustable viewing geometry [9]. An adjustable sensor swivels from side to side or back and forth. This is extremely important for repeat imaging and stereo capabilities.

Most electro-optical satellites are synchronized with the Sun so they make repeat passes over a particular area at the same time of the day. This ensures that Sun angle and shadowing will be similar in multiple images acquired over the same area on different orbits. Most satellite orbits have mid-morning equatorial crossings so that images are captured when the sun angle is low. Thus the resultant Sun shadows do not obscure terrain relief.

Satellite imagery are processed in order to enhance their geometric accuracy as well as their visual appearance. Several processing levels are available by the image supplier. The customer should determine the processing level he will require. This choice depends basically on the type of software available for processing the imagery. There are generic terms for the common processing classes [11]. Suppliers have their own product names that are equivalent to such terms. Raw class is the lowest level of processing. Here, the images are corrected for some geometric and radiometric distortions. Distortions due to the satellite sensor are eliminated in this level. In Geometric Correction class, the image is resampled in order to correct for geometric distortions due to Earth rotation and sensor incidence angle.

Using position information recorded by the satellite at the time of image capture, image data are converted to cartographic coordinates and then the projection system selected by the customer to provide the so called Basic GeoCoded class. In Fully GeoCoded class, image data are corrected using ground control points. Ground control is obtained using available maps or GPS measurements and sometimes is provided by the customers. OrthoRectified class means that horizontal as well as vertical image distortions are eliminated utilizing digital elevation models. As a result, the geometric quality of the image gains significant improvement and reaches the map quality. Some enhancement techniques, such as contrast stretching, are applied to the imagery in order to increase the image quality and highlight certain features, leading to the Enhanced class of satellite imagery.

2. Image Correction and Enhancement

Raw satellite images always have geometric distortions and often have radiometric distortions. Such problems have to be corrected or minimized using image and enhancement techniques. Three types of geometric distortions exist in raw images. Firstly, distortions related to sensor position, orientation and geometry. Secondly, distortions introduced by terrain relief. Lastly, distortions caused by orientation of satellite images relative to the map coordinate system. All three types of geometric distortion require resampling of the raw images [10].

Regarding sensor distortions, some of them are common to all types of imagery. Examples are atmospheric refraction and panoramic distortion. In panoramic imagery, pixels at the center of an image are smaller than near its margins. Other sensor distortions are unique to a particular type of sensor. One example is shearing of satellite images caused by Earth rotation during acquisition of consecutive scan lines.

The distortion introduced by terrain relief causes displacement of individual pixels in the image plane from their expected position on the map. The magnitude of the displacement is a function of the image and sensor geometry, pixel position within the image, and terrain elevation at the point. For nearly vertical, low-resolution imagery this type of distortion can be reduced using simple polynomial warping of images. This approach would not be suitable for high-resolution or non-vertical imagery, where relief displacement can be hundreds of pixels. To remove the distortion in such imagery, terrain elevation at every pixel of the output image should be known. A Digital Elevation Model (DEM) is the most suitable form to provide these data.

Projection distortion is caused by the arbitrary orientation of raw images with respect to the map coordinate system. Prior to their use in information extraction stage, the images are to be converted to a desired coordinate system and aligned with it's axes. This operation usually involves rotating and scaling of images, but sometimes might require more complex, non-linear transformation.

Geometrically corrected images may be still not suitable for visual analysis and interpretation due to their poor radiometric appearance. Radiometric correction and enhancement improves the appearance of images by modifying their histograms. When several images are to be combined to cover large area, it is necessary to adjust their appearance in order to make the seams less obvious. This process is called histogram balancing. More sophisticated radiometric enhancement approaches takes into account optical properties of the atmosphere and of the imaging sensor to model the distortion of the signal between the reflecting surface and the sensor. They may also consider factors as dust, water vapor or aerosols suspended in the atmosphere, terrain elevation, slope and aspect, and solar illumination angles.

3. Extracting Information from Satellite Imagery

In this stage, a description of the image content is obtained through the analysis of the variation in pixel intensity values across the image. Image classification, vector digitization and feature extraction are some of the processes that can be performed in this regard. Although most features appearing in IKONOS imagery can be derived using image-based vector digitization, extensive field verification would be required to evaluate and fix the errors in the image interpretation.

The purpose of image classification process is to divide an image into a number of non-overlapping regions, based on their spectral properties. Each classified region represents certain land cover type, such as urban, water, forest, ...etc. Finer classifications can be possible according to the spatial as well as the spectral resolution of the imagery. Image classification algorithms are aggregated into two classes; supervised and unsupervised. Supervised classification is performed in accordance with the guidance of the operator, whereas unsupervised classification is a fully automatic process [9].

Image-based vector digitization aims at deriving shapes and other properties of linear features, such as roads, railways and drainage patterns. Areas, such as lakes and boundaries of urban areas can also be traced at this process. Vector digitization is mainly performed manually. It is sometimes assisted by automatic feature extraction. Here an automatic line following software is used for delineating the linear features.

However, ambiguous circumstances can not be resolved without a human operator. It is worth-mentioning that automatic feature detection works well at identification of features of known or assumed shapes.

It is worth-mentioning that the accuracy of image-based digitization depends mainly on the image resolution as well as the level of clearness of the features to be digitized. In the matter of fact, different image features have different degrees of clarity and thus different definition errors are resulted. As the image resolution gets finer, definition errors for most features can be kept at minimum level.

4. IKONOS Imagery

Developed by Space Imaging, IKONOS-2 is scheduled for launch in late 1999. IKONOS-1 was launched on April 27, 1999, but failed to achieve orbit. IKONOS-2 is designed to occupy a 681-km sun-synchronous orbit having an equatorial crossing time of 10:30 am. The ground track of the system repeats every 11 days, but the revisit time (time elapsing between passes) for imaging is less than 11 days, based on latitude and the tilt of the system selected to acquire any given image [8]. The system has the capability to collect data at angles of up to 45° from vertical both in the across-track and along-track directions. At nadir, the swath width of the system is 11 km. A typical image is 11 km by 11 km, but user-specified strips can also be obtained.

A linear array technology is adopted by the IKONOS system. Here the array of detectors typically consists of numerous charge-coupled devices (CCDs) positioned end to end. Each spectral band of sensing has its own linear array. The resolution of the panchromatic sensor is one meter whereas the resolution of the multispectral scanner is four meters. IKONOS Bands and Frequencies are blue (0.45 μm to 0.52 μm), green (0.52 μm to 0.60 μm), red (0.63 μm to 0.69 μm), Near IR (0.76 μm to 0.90 μm), and Pan (0.45 μm to 0.90 μm). A great advantage of the IKONOS system is its being highly maneuverable. Within a few seconds, the system can point to a certain target and stabilize itself. Moreover, the system can be programmed to follow many features including winding features.

In a one-meter resolution image, objects that are one-meter in size on the ground can be distinguished, such that those objects are well removed from other objects and have distinct visual characteristics. For example, objects such as cars, trucks, boats, and swimming pools can easily be detected. Such objects are recognizable because of their correlation with their surroundings. Comparable with the ten-meter SPOT imagery and the five-meter IRS imagery, one-meter IKONOS images give the user much greater capability to discern many types of objects.

5. The Case Study

The test image (Fig.1a) of this study is a panchromatic IKONOS digital image of 1m ground resolution for Maadi district, Cairo. It is captured on April 17, 2000 and corrected for geometric distortions due to the satellite sensor as well as Earth rotation. The image data are geocoded (converted to cartographic coordinates) using position information recorded by the satellite at the time of image capture. The image shows some urban areas, part of the ring road around Cairo, and part of Mokatam hill.

The main goal of the experimental work is to evaluate the effect of various image distortions, excluding relief distortion, on the accuracy of measured coordinates of image points as well as measured distances between the points. Such evaluation would provide good indication to the accuracy of image-based vector digitization of IKONOS imagery. Based on the reconnaissance of the test area, a set of twenty-two well-identified feature points is selected carefully in the test image such that they almmst have the same height. This would ensure that relief has an insignificant effect. Most of the selected features are corners of buildings and other structures. The image coordinates of the feature points are measured in the pixel coordinate system using an image processing software.

A terrestrial surveying work is accomplished to get the object coordinates of the selected points in an arbitrary ground coordinate system. Unfortunately, some (ten) of the selected points were not accessible and could not be surveyed. Actually, these points are located inside governmental places and thus a special permission is required in advance to reach them. The accessible twelve points (Fig. 1b) have been observed using the Total Station Sokkia Set 2C, with a precision of ±(2-3 mm)+2 ppm. In addition,

ground measurements have been made to get the widths of some roads and streets, and the dimensions of some planar objects. The corresponding image measurements are derived using the image processing software.

Three 2-D transformation models are used in this study to assess the accuracy of point positioning in the test image. These models are similarity transformation, affine transformation, and projective transformation. Similarity transformation requires at least two known points to solve for its four parameters; one scale, one rotation and two shifts. This transformation is given by

$$x_t = a\,x + b\,y + c \quad \ldots\ldots (1)$$

$$y_t = -\,b_1\,x + a\,y + d \quad \ldots\ldots (2)$$

In affine transformation, two more parameters are included; one additional scale and one skew factor. Here a minimum of three known points is a must to solve for the six transformation parameters. The transformation is defined by these two equations

$$x_t = a\,x + b\,y + c \quad \ldots\ldots (3)$$

$$y_t = d\,x + e\,y + f \quad \ldots\ldots (4)$$

A projective transformation is an eight-parameter transformation, which describes the central projectivity between two planes [3]. It is given by

$$x_t = (a_1\,x + b_1\,y + c_1) / (a_0\,x + b_0\,y + 1) \quad \ldots\ldots (5)$$

$$y_t = (a_2\,x + b_2\,y + c_2) / (c_1\,x + c_2\,y + 1) \quad \ldots\ldots (6)$$

At least four known points are to be available to carry out the projective transformation.

The Direct Linear Transformation (DLT) is another mathematical model that relates image coordinates to object coordinates through eleven parameters. It transforms coordinates from a 3-D space to 2-D space. The accuracy of the transformation is sensitive to the configuration of control points in the object space, especially in the camera-axis direction. DLT would not be suitable to be applied in our test since the selected feature points are almost planar.

6. Results and Analysis

The image coordinates of the feature points are measured in the pixel coordinate system using the image processing software. The software enables the user to get coordinates

with a resolution of a fraction of a pixel. Transformed image coordinates are computed using similarity, affine and projective transformations. In each transformation, some of the twelve ground control points are utilized whereas the rest of them are used as check points. Considering that the control points are error free, the results of the transformation provide an indication for the accuracy of the point positioning of single IKONOS imagery. Tables 1-3 report statistics of the differences among measured and transformed coordinates of the check points by similarity, affine and projective transformations; respectively. Each table lists RMS, mean, and maximum values of the resulted differences in each of the x-coordinates and y-coordinates, beginning by the minimum control points and reaching six control points. The tables show that the RMS values are below one meter. This means that the planimetric coordinate accuracy for the selected feature points is better than the image resolution.

Comparing the figures included in the tables mentioned above, it could be drawn that the results achieved by each of the three transformations are close to the corresponding results reached by the other two transformations. However, similarity transformation has the advantage that it requires the minimum number of control points (only two). It is also noticed that while configuring control points improperly has undesired influence on the results of affine and projective transformations, it has no influence on similarity-transformation results.

The distances among selected points, derived from their measured image coordinates as well as from their transformed coordinates, are compared with the corresponding distances inferred from ground coordinates. Table 4 illustrates the estimated distances in the case of using five control points. Table 5 includes statistics of the differences among ground coordinates and each of the Image and transformed coordinates. For the differences among image and ground distances, the RMS is 1.317 m. The average of their absolute values is found to be 1.062 m whereas their maximum value is 2.972 m. These figures get better for the differences among transformed and ground distances. As illustrated in Table 5, RMS values reaches 0.870 m in the case of similarity transformation.

According to the proposed accuracy standards of the American Society of Photogrammetry and Remote Sensing, for a map scale of 1:4,000, the planimetric coordinate accuracy (RMSE in either the x- or y-coordinate) of map points should reach one meter [1]. Therefor, the estimated planimetric accuracy of selected test points leads to the conclusion that a map scale of 1:4,000 could be produced by digitizing of well-defined features in single IKONOS imagery. Here, errors that might occur in the phase of map compilation subsequent to the digitization phase are disregarded.

In regard to the amount of relief distortion for objects in the test image, it is found that it reaches about one third of the object height. This significant magnitude of relief distortion is due to that the test image is an oblique image. In an oblique imagery, the distance from an image point to the sensor nadir point gets much larger than in vertical or near-vertical imagery, depending on the degree of inclination of the sensor. Such a distortion causes great difficulties in the determination of correct locations of elevated objects as well as correct distances among objects having different heights. Therefore, an oblique image is to be rectified to get vector digitization results.

In respect of the identification of roads and streets, it is found that roads and major streets are clearly identifiable and adequately visible. In addition, minor streets having less width are generally discernible. However, the reflectance of some minor streets and that of the adjoining buildings merge at some places which complicates the identification of the street. In fact, identification of streets passing through open areas is easier than in built-up areas because of their relief distortion. It is found also that the measurements of road width and planar-object dimensions, as obtained from the image, are very close from their corresponding measurements attained by terrestrial surveying. The differences are less than the resolution of the image.

7. Conclusions

This research aims at investigating the potential of the attainable planimetric accuracy of ground points from single IKONOS imagery. The test image is a recent panchromatic IKONOS digital image of 1m resolution and corrected for geometric distortions due to

the satellite sensor as well as Earth rotation. As a matter of fact, this image belongs to the first processing level of IKONOS imagery.

In order to achieve the research goal, the planimetric coordinate accuracy of a set of selected feature points in the test image is assessed by using three transformation models. In addition, the accuracy of linear measurements in the test image is evaluated. Here, image distances derived among the feature points are tested against their corresponding ground distances attained by terrestrial surveying. The accuracy of those image distance are further investigated after transformation. Based on the achieved test results, the following conclusions can be made;

1. The planimetric coordinate accuracy of well-defined feature points in IKONOS imagery reaches a magnitude that is less than the image resolution.
2. Similarity transformation requires less control and gives almost equivalent results comparing with affine and projective transformations.
3. Regardless of relief distortion, the accuracy of measured distances in the image among well-defined feature points exceeds the image resolution with a slight amount.
4. The accuracy of those image distances gets better after transformation and reaches the image resolution.
5. Considering the proposed accuracy standards of the American Society of Photogrammetry and Remote Sensing, a map scale of 1:4,000 could be obtained from the digitization of well-identified features in single IKONOS imagery. Here, other errors that might result in map compilation phases following after digitization are overlooked.

Finally, since relief distortion could be of significant magnitude in oblique IKONOS imagery, it is necessary to continue research toward reduction of such a distortion to insure good digitization results. The question to be answered here is how to incorporate the relief deformation into suitable polynomial-based geometric correction models in order to apply them for image rectification.

References

[1] **Anderson, J.M. and Mikail, E.M.** (2001) "Surveying: Theory and Practice", The McGraw-Hill companies, Inc., New York.

[2] **Ajayi, G.E.** (1992) "Topographic Mapping From Satellite images: How Feasible in Developing Countries?" International Archives of Photogrammetry and Remote Sensing, Vol. XXIX, Part B4.

[3] **Blais, J.A.** (1994) " Map projection and Cartography" Class Notes, Department of Geomatics Engineering, University of Calgary, Calgary, Alberta.

[4] **Colwell, Robert N.** (1983) "Manual of Remote Sensing" Falls Church, Virginia: American Society of Photogrammetry.

[5] **Drachal J. and Kaczynski, R.** (2001) "The New Approach to Processing of High Resolution Image Data Applied to Image Maps in Scales from 1:10,000 to 1:50,000" International Archives of Photogrammetry and Remote Sensing, Vol. XXI, Part B4.

[6] **Folchi, W.** (1996) "Satellite Orthoimagery: Mapping the Future Today, The Space Imaging Approach, Proceedings of ACSM/ASPRS Annual Conference, Baltimore, MD, Vol. 2.

[7] **Fritz, L.W.** (1996) "Commercial Earth Observation Satellites" International Archives of Photogrammetry and Remote Sensing, Vol. XXXI, Part B4.

[8] **IKONOS** (2001) "Information about the IKONOS Satellite and 1-m Panchromatic and 4-m Multispectral data" http://www.spaceimaging.com/products/IKONOS.html.

[9] **Lillesand T. and Kiefer R.** (2000) " Remote Sensing and Image Interpretation" John Wiley & Sons, Inc., New York.

[10] **Novak, K.** (1994) "Photogrammetric Mapping" Class Notes, Geodetic Science Department, Ohio State University.

[11] **SPOT Image Corporation** (1998) "Satellite Imagery: An Objective Guide" SIC, Reston, Virginia.

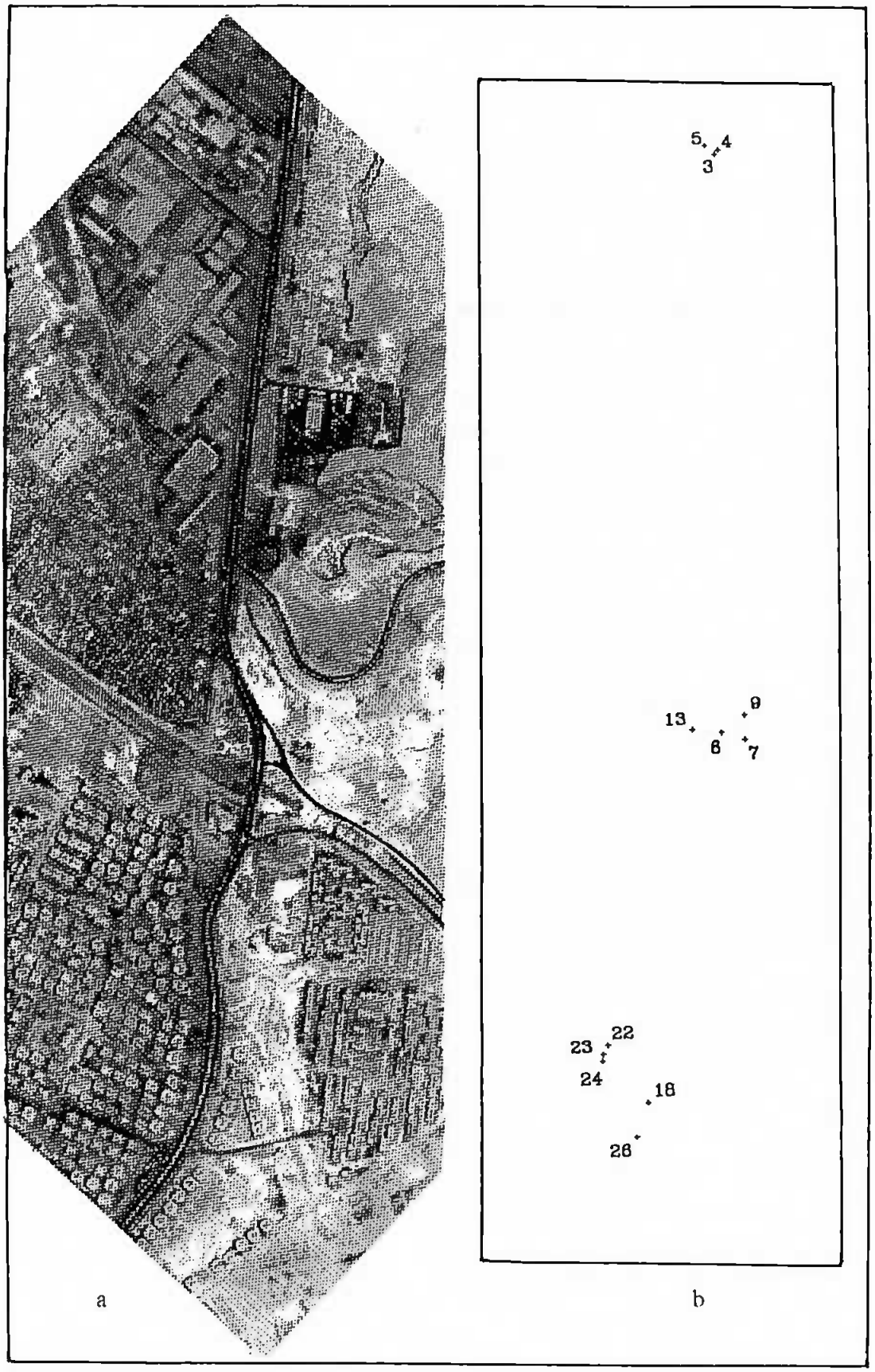

Figure 1: a) The Part of The IKONOS Image Which includes The Test Area
b) The Distribution of Observed feature Points in The Test Area

Table 1: Statistics of The Differences Among measured And Transformed Coordinates at Using Similarity Transformation, in Meters

	Root Mean Square		Average		Maximum	
	X	Y	X	Y	X	Y
2 Control Pts.	0.991	0.703	0.836	0.539	1.885	1.650
3 Control Pts.	0.875	0.695	0.779	0.520	1.492	1.583
4 Control Pts.	0.773	0.656	0.672	0.485	1.344	1.457
5 Control Pts.	0.695	0.635	0.573	0.414	1.341	1.362
6 Control Pts.	0.642	0.529	0.594	0.374	1.266	0.606

Table 2: Statistics of The Differences Among measured And Transformed Coordinates at Using Affine Transformation, in Meters

	Root Mean Square		Average		Maximum	
	X	Y	X	Y	X	Y
3 Control Pts.	0.841	0.691	0.753	0.523	1.412	1.544
4 Control Pts.	0.736	0.674	0.691	0.499	1.002	1.443
5 Control Pts.	0.721	0.630	0.669	0.425	0.965	1.369
6 Control Pts.	0.707	0.462	0.618	0.410	1.023	1.089

Table 3: Statistics of The Differences Among measured And Transformed Coordinates at Using Projective Transformation, in Meters

	Root Mean Square		Average		Maximum	
	X	Y	X	Y	X	Y
4 Control Pts.	0.865	0.881	0.880	0.772	1.268	1.462
5 Control Pts.	0.771	0.604	0.721	0.527	1.135	1.078
6 Control Pts.	0.770	0.575	0.716	0.500	1.039	1.010

Table 4: Image, Transformed and Ground Distances Among Control and Check Points, in Meters

From	To	Image	Projective	Affine	Similarity	Ground
3	4	11.285	11.905	11.523	11.518	11.527
3	5	25.551	25.487	26.128	26.234	26.254
3	6	1180.972	1181.806	1180.288	1180.698	1181.606
3	7	1196.561	1196.685	1195.952	1196.567	1197.487
3	9	1147.613	1147.023	1146.416	1147.012	1147.894
3	13	1177.146	1177.815	1175.233	1175.406	1176.310
3	18	1937.898	1939.378	1938.367	1938.424	1939.914
3	22	1834.096	1833.566	1832.409	1832.155	1833.563
3	23	1851.656	1852.627	1851.656	1851.376	1852.799
3	24	1884.700	1884.840	1884.183	1883.875	1885.323
3	26	2010.032	2010.164	2009.718	2009.711	2011.256
4	5	28.858	28.225	28.503	28.622	28.644
4	6	1188.922	1190.944	1188.967	1189.348	1190.263
4	7	1204.191	1205.516	1204.329	1204.914	1205.840
4	9	1155.230	1155.844	1154.783	1155.349	1156.237
4	13	1185.488	1187.321	1184.279	1184.425	1185.336
4	18	1946.464	1949.096	1947.623	1947.656	1949.153
4	22	1843.006	1843.604	1841.988	1841.712	1843.127
4	23	1860.595	1862.689	1861.260	1860.958	1862.388
4	24	1893.661	1894.925	1893.810	1893.480	1894.936
4	26	2018.664	2019.942	2019.036	2019.005	2020.557
5	6	1197.616	1198.196	1197.797	1198.295	1199.216
5	7	1213.946	1213.824	1214.199	1214.907	1215.841
5	9	1165.036	1164.195	1164.695	1165.384	1166.280
5	13	1192.801	1193.215	1191.760	1192.015	1192.932
5	18	1952.848	1954.067	1954.183	1954.317	1955.820
5	22	1848.038	1847.242	1847.206	1847.021	1848.441
5	23	1865.507	1866.220	1866.369	1866.158	1867.593
5	24	1898.480	1898.353	1898.814	1898.575	1900.034
5	26	2024.788	2024.661	2025.342	2025.411	2026.968
6	7	49.250	49.181	49.056	49.261	49.299
6	9	58.240	58.898	58.043	58.056	58.100
6	13	59.449	59.178	59.028	59.245	59.291
6	18	766.913	767.519	767.994	767.713	768.303
6	22	680.487	679.112	679.538	679.089	679.611
6	23	699.342	699.257	699.880	699.415	699.952
6	24	732.893	732.185	733.129	732.642	733.205
6	26	840.758	839.986	841.030	840.699	841.345

to be continued,

Table 4 (continued)

7	9	48.989	49.689	49.563	49.582	49.620
7	13	108.090	107.848	107.577	108.001	108.084
7	18	763.818	765.126	764.714	764.319	764.907
7	22	684.927	684.271	683.834	683.340	683.865
7	23	703.988	704.544	704.305	703.795	704.336
7	24	737.358	737.361	737.442	736.910	737.476
7	26	838.066	837.992	838.149	837.707	838.351
9	13	110.150	109.989	108.853	109.072	109.156
9	18	811.126	813.023	812.497	812.106	812.731
9	22	729.784	729.625	729.066	728.553	729.113
9	23	748.777	749.858	749.497	748.968	749.544
9	24	782.235	782.738	782.698	782.147	782.748
9	26	885.298	885.810	885.853	885.414	886.095
13	18	762.215	763.034	764.604	764.499	765.087
13	22	667.267	666.111	667.594	667.248	667.761
13	23	685.749	685.971	687.649	687.284	687.812
13	24	719.312	718.831	720.829	720.442	720.996
13	26	835.204	834.661	836.799	836.637	837.280
18	22	138.102	139.638	140.141	140.596	140.704
18	23	131.663	131.463	131.948	132.443	132.545
18	24	119.058	119.767	120.289	120.805	120.898
18	26	74.372	72.992	73.561	73.515	73.571
22	23	19.194	20.302	20.500	20.485	20.501
22	24	52.451	53.114	53.632	53.594	53.635
22	26	191.318	192.040	192.910	193.248	193.396
23	24	33.586	32.932	33.253	33.231	33.257
23	26	179.100	178.137	178.895	179.281	179.419
24	26	154.665	154.878	155.470	155.913	156.033

Table 5: Statistics of The Differences Among Ground Coordinates and Each of The Image and Transformed Coordinates, in Meters

Stat.	Gr. -Im.	Gr. - Proj.	Gr. - Aff.	Gr. - Simi.
RMS	1.317	1.055	0.901	0.870
Ave.	1.062	0.819	0.681	0.694
Max.	2.972	2.619	1.642	1.557